hydrogen

Article

Integration of Wind Energy and Geological Hydrogen Storage in the Bakken Formation, North Dakota: Assessing the Potential of Depleted Reservoirs for Hydrogen Storage

Shree Om Bade [1,*], Emmanuel Gyimah [1,*], Rachael Josephs [1], Toluwase Omojiba [1], Rockson Aluah [2] and Olusegun Stanley Tomomewo [1,*]

[1] Department of Energy Engineering, University of North Dakota, Grand Forks, ND 58202, USA
[2] Department of Petroleum Engineering, University of North Dakota, Grand Forks, ND 58202, USA
* Correspondence: shree.bade@und.edu (S.O.B.); emmanuel.gyimah@und.edu (E.G.); olusegun.tomomewo@und.edu (O.S.T.)

Abstract: Geological hydrogen storage, seen as a viable solution for addressing energy demands and mitigating the intermittency of wind power, is gaining recognition. At present, there are no specific studies that estimate hydrogen storage capacity and the potential for wind integration in North Dakota despite the state's enormous energy resources and capabilities. The study's key innovation lies in repurposing a region historically associated with oil and gas for sustainable energy storage, thereby addressing the intermittency of wind sources. Moreover, the innovative aspect of this study involves field selection, site screening, characterization, and mathematical modeling to simulate a wind–hydrogen production and geological storage system. A 15 MW wind farm, using real-world data from General Electric wind turbines, is employed to assess storage capacities within the Middle Bakken formation. The study reveals substantial storage potentials in wells W24814, W19693, and W26990, with capacities of 54,000, 33,000, and 22,000 tons, respectively. These capacities translate to energy storage capabilities of 1080, 660, and 440 GWh, with minimum storage durations of 140, 80, and 57 days, respectively, under a 60% system efficiency. By pioneering the integration of wind energy with geological hydrogen storage in a region traditionally dominated by fossil fuel extraction, this research could play a crucial role in advancing North Dakota's energy transition, providing a blueprint for similar initiatives globally.

Keywords: underground hydrogen storage; wind energy; hydrogen production; depleted oil and gas reservoir

Citation: Bade, S.O.; Gyimah, E.; Josephs, R.; Omojiba, T.; Aluah, R.; Tomomewo, O.S. Integration of Wind Energy and Geological Hydrogen Storage in the Bakken Formation, North Dakota: Assessing the Potential of Depleted Reservoirs for Hydrogen Storage. *Hydrogen* **2024**, *5*, 737–760. https://doi.org/10.3390/hydrogen5040039

Academic Editor: Adolfo Iulianelli

Received: 20 July 2024
Revised: 28 August 2024
Accepted: 15 October 2024
Published: 17 October 2024

1. Introduction

Renewable energy sources like solar and wind power have gained significant attention due to their abundant potential and minimal environmental impact [1,2]. However, the intermittent and variable nature of renewables necessitates effective storage solutions to ensure a stable and reliable energy supply [3,4]. Hydrogen (H_2) storage offers a complementary solution, providing high-energy density storage that batteries alone cannot achieve [5]. The global community is increasingly embracing H2 as a sustainable solution to reduce its carbon footprint [6], and various sectors such as transportation, industrial processes, power generation, and residential heating can utilize H_2-based economies that align with renewable energy trends. The need for greenhouse gas abatement [7,8], technological advancements [9,10], governmental commitments [11], targets from leading industry actors [12], and various policy frameworks in conjunction with international endeavors are driving this transition [13].

Several methods for H_2 generation exist, with steam methane reforming (SMR), electrolysis, and gasification being the main processes globally [10,12]. One of the more readily deployed is SMR, which uses natural gas (blue H_2 or gray H_2) and electrolysis fueled by renewable energy (green H_2). To mitigate challenges associated with H_2 generation and foster large-scale deployment of renewable energies, a highly competitive, scalable, safe, and environmentally friendly energy storage solution is indispensable. H_2 is positioned as one of the best-suited options [14].

To accommodate the surplus H_2 being produced, large-scale H_2 storage facilities need to be constructed. Underground hydrogen storage (UHS) has gained significant attention due to its cost-effectiveness, scalability, safety, and extensive storage capacity, often surpassing surface storage methods by orders of magnitude [15–17]. Underground reservoirs (Figure 1), such as depleted oil and gas formations, aquifers, and salt caverns, provide substantial storage capacity with minimal environmental impact, making them attractive options for large-scale energy storage (Figure 2) [18,19].

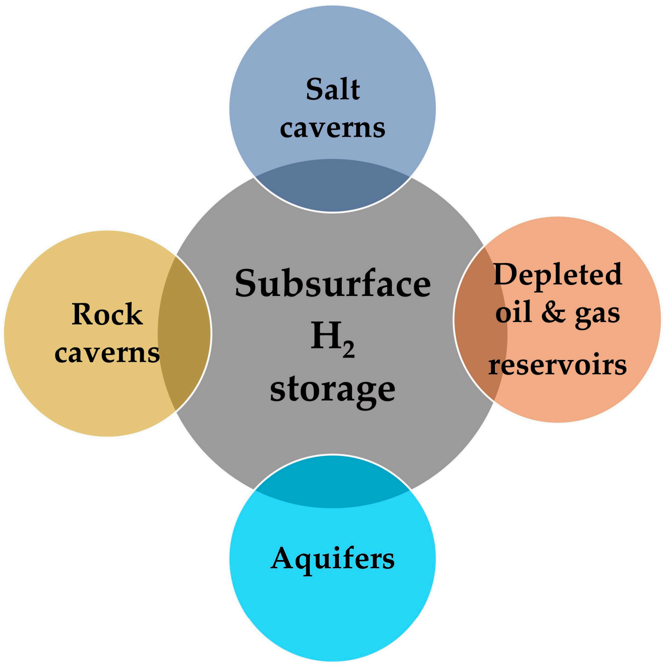

Figure 1. Geological hydrogen storage.

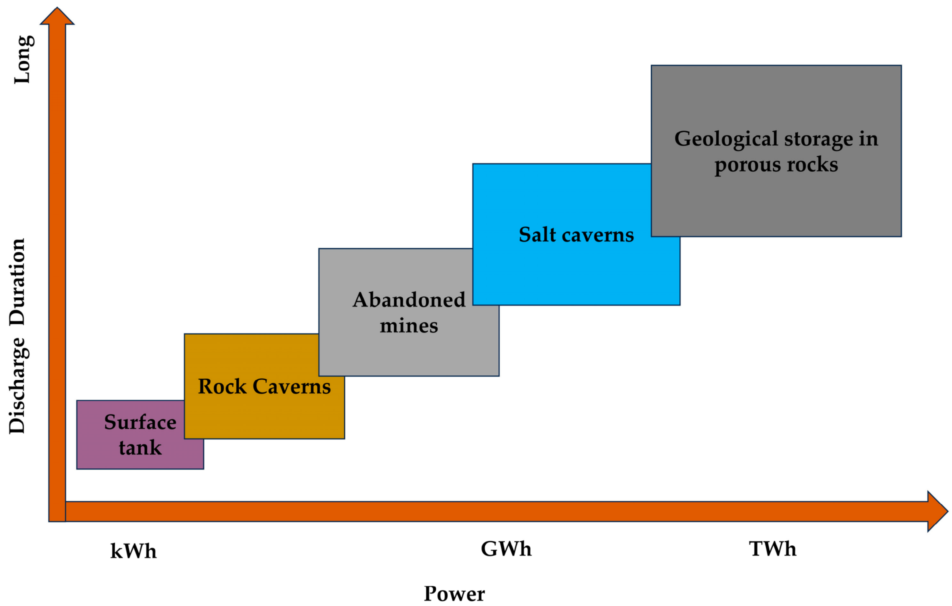

Figure 2. Scalability of hydrogen storage in various confining media.

Several UHS projects are now reported to have been successfully operated through an increasingly number of studies (Table 1) [16,20], which is promising for the future use of UHS as a long-duration, large-scale H_2 storage technology. It involves selecting suitable geological reservoirs based on physical-chemical properties, reservoir tightness, and geochemical interactions [20]. While it is synonymous with CO_2 storage, H_2 storage is typically short-term and has different physical-chemical requirements compared to CO_2 storage [21].

Table 1. Worldwide active UHC Sites [17,20].

Country	Field/Project Name	H_2 (%)	Pressure Conditions	Depth (m)	Volume (m^3)	Status
			Depleted reservoir			
Argentina	Diadema	10	10 bar/50 °C	600	Not reported	Operating
Austria	Underground Sun Storage	10	78 bar/40 °C	1000	Not reported	Operating
Argentina	Hychico	10	-	600–800	Not reported	Operating
Russia	Yakshunovskoe field	-	-	-	-	Operating
			Aquifers			
Czech Republic	Lobodice	50	90 bar/34 °C	430	Not reported	Operating
France	Beynes	50	Not reported	450	3.3×10^6	Operating with natural gas
			Salt Caverns			
United Kingdom	Teesside	95	45 bar	365	210,000	Operating
United States	Clemens	95	70–137 bar	1000	580,000	Operating
	Moss Bluff	95	60–100 bar	1200	566,000	Operating
	Spindletop	95	68–202 bar	1340	906,000	Operating
Germany	Kiel	60	50–100 bar	1330	32,000	Repurposed as natural gas storage
	Bad Lauchstädt, Town gas	-	-	800	6.7×10^8	Repurposed as natural gas storage
	Kirchhellingen, Town gas	-	-	900	2.4×10^8	Repurposed as natural gas storage
	Hähnlein, Town gas	-	-	500	1.6×10^6	Repurposed as natural gas storage

The U.S. government is currently implementing strategies to incorporate H_2 into the national energy system, with a strong focus on clean H_2 [13]. As experts in national energy planning predict a rapid growth in wind energy generation, using wind-generated electricity to produce green H_2 for export could play a crucial role in making H_2 an economically viable energy carrier for the country [22]. Measures such as establishing H_2 storage in geological reservoirs are necessary to ensure sufficient hydrogen for export and enhance the security of the United States (U.S.) electricity sector. The U.S. Bureau of Economic Geology identifies dissolution cavities in salt domes, depleted oil and gas fields, and brine reservoirs as viable options for large-scale geological storage (Figure 3). However, further research and development are required to create a more extensive inventory of suitable storage locations throughout the United States. Table 2 provides an overview of large-scale UHS in the United States.

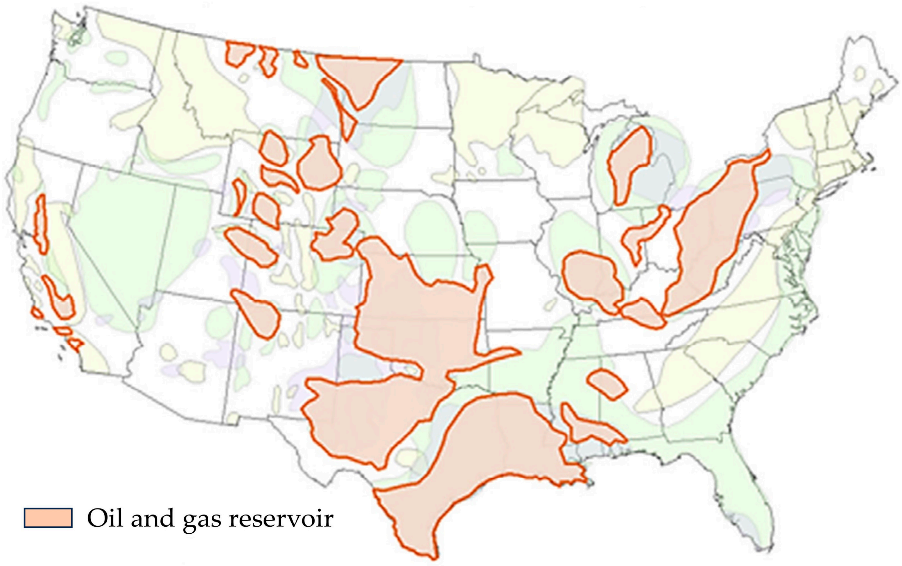

Figure 3. Illustrating oil and gas reservoirs in the USA (image: modified from [23]).

Table 2. Large-scale geological storage of hydrogen in the U.S. [24].

Type	Status	Comments
Salt caverns	3 active storage projects in Texas for industrial use	Limited geographic distribution
Depleted oil and gas fields	Untested for H_2 storage	Wide geographic distribution
Saline aquifers	Untested for H_2 storage	Wide geographic distribution. Suitability of sealing caprocks

However, UHS is a relatively new field that is expected to significantly impact its long-term energy carrier viability. It involves selecting suitable geological reservoirs based on physical-chemical properties, reservoir tightness, and geochemical interactions [20]. While it is synonymous with CO_2 storage, H_2 storage is typically short-term and has different physical-chemical requirements compared to CO_2 storage [21].

The U.S. government is currently implementing strategies to incorporate H_2 into the national energy system, with a strong focus on clean H_2 [13]. Concurrently, experts in national energy planning predict a rapid growth in wind energy generation [22]. As a result, using wind-generated electricity to produce green H_2 for export could play a crucial role in making H_2 an economically viable energy carrier for the country. Moreover, to ensure sufficient hydrogen for export, and enhance the security of the U.S. electricity sector, measures such as establishing H_2 storage in geological reservoirs are necessary. The U.S. Bureau of Economic Geology identifies dissolution cavities in salt domes, depleted oil and gas fields, and brine reservoirs as viable options for large-scale geological storage (Figure 3). However, further research and development are required to create a more extensive inventory of suitable storage locations throughout the United States. Table 2 provides an overview of large-scale UHS in the United States.

Furthermore, among the available options, depleted oil and gas reservoirs have gained attention due to their well-understood geological structures, high density, intact source rock, and existing surface and subsurface infrastructure [25]. They have proven to be a cost-effective solution [1] and offer H_2 storage capacities several times larger than other types (Figure 3) when comparing discharge duration and power [26]. Table 3 provides typical selection criteria for depleted hydrocarbon reservoirs.

Table 3. General UHS criterion for depleted hydrocarbon reservoirs [14,20].

Criteria	Requirement
Geology rock type	Large sedimentary rocks, massive non-foliated metamorphic rocks, and intrusive igneous rocks
Structure	Isotropic rocks: Rocks poorly falter, no discontinuities, fissured, deformations, homogenous, jointed, and folded; no significant tectonic
Porosity	Low
Hydraulic conductivity	<10^8 m/s for H_2O
Depth	70–200 m
Permeability	Low
Lifecycle	>30 years
Thermal stability	4 to 80 °C

This study investigates the use of depleted gas fields for H_2 storage, in the Bakken Formation situated in North Dakota's Williston Basin, utilizing the extensive technical expertise developed in the U.S. and other regions as a case study. The Bakken Formation, a significant geological formation in North Dakota, offers considerable potential for H_2 storage. Known primarily for its oil and gas reserves, the Bakken Formation's unique geological characteristics also make it suitable for H_2 storage. As of November 2022, there were 17,563 active oil and gas wells in production in North Dakota [26]. Moreover, North Dakota ranks among the top states in the U.S. for wind power capacity due to its substantial wind energy resources [27]. The state's vast open plains and favorable wind conditions make it an ideal location for wind energy generation. Despite the considerable installed wind capacity, the variability in wind speeds poses challenges for maintaining a consistent power supply. Hence, integration with H_2 storage could significantly improve the reliability and efficiency of wind energy systems in North Dakota.

By leveraging the region's favorable geological characteristics and substantial wind resources, North Dakota can pioneer an integrated energy system that not only bolsters energy security but also contributes to the state's shift towards a more carbon-neutral and resilient energy infrastructure. This research aims to identify optimal locations within the Bakken Formation for subsurface H_2 storage and evaluate the feasibility of large-scale wind–H_2 integration, providing valuable insights for the development of sustainable energy policies and strategies.

At present, there are no specific studies that estimate the H_2 storage capacity of the Williston Basin. The novelty of this research lies in the comprehensive integration of wind energy with geological H_2 storage, specifically within the Bakken Formation in North Dakota, with one strategy to consider the use of local strengths and resources. For instance, North Dakota with abundant wind energy resources can focus on green H_2 production, in addition to blue H_2 with carbon capture and storage; however, the scope of this work is based on green H_2 production. While H_2 storage and wind energy are not new concepts, combining these technologies in the context of an established geological formation primarily known for its oil and gas reserves is innovative. To the author's knowledge, this study is the first to introduce a large-scale geological storage system integrated with wind-generated H_2. The motivation for this study stems from a paucity of adequate literature in this knowledge area, specifically pertaining to North Dakota. The objectives of this study are twofold. Firstly, it aims to identify suitable locations within the Bakken Formation for subsurface H_2 storage using readily available data from existing wells from the North Dakota Department of Mineral Resources (NDDMR). Secondly, it aims to evaluate the possibility of large-scale wind–H_2 storage in depleted oil and gas fields. To achieve these objectives, a comprehensive methodology is employed, which includes field selection, reservoir characterization, and mathematical modeling to simulate the wind, H_2 production, and storage systems. This study contributes to the existing knowledge on hydrogen storage in depleted oil and gas reservoirs. Additionally, it sheds light on the potential of geological hydrogen storage as a crucial component in integrating renewable energy sources with the current energy infrastructure. The findings and insights from this research can inform the development of sustainable energy policies and strategies, facilitating the shift to a more carbon-neutral and resilient energy system. Furthermore, it contributes to the discussion on whether depleted oil and gas reservoirs can serve as H_2 storage technology in the future, underscoring the importance of hydrogen as a potential energy vector.

The subsequent sections of the paper provide a brief literature overview, outline the methodology and mathematical models used, present the data and assumptions utilized in the study, and discuss the results and implications of the analysis. Finally, the paper concludes with remarks and recommendations for further research in this field.

2. Related Studies on Underground Hydrogen Storage in Depleted Gas Reservoirs

Although the integration of renewable sources and storage of large amounts of H_2 (ranging from tens to thousands of tons) has received attention, very limited literature is available. Currently, successful storage of H_2 in underground geological formations is mainly limited to aquifers and caverns in Europe and the United States, as indicated in Table 1 [1]. This study does not aim to provide an exhaustive list and analysis of all H_2 storage sites. Instead, it focuses on highlighting advancements in UHS worldwide, particularly in terms of their potential and large-scale feasibility for depleted reservoirs. For example, Tarkowski [28] conducted a comprehensive review of the geological aspects of hydrogen storage in depleted gas fields. The study emphasized the importance of reservoir characterization parameters such as porosity, permeability, and cap rock integrity in determining the suitability of a depleted reservoir for hydrogen storage. Zivar et al. [17], explored the potential of depleted gas reservoirs for hydrogen storage in the context of the energy transition. They provided a framework for assessing the suitability of specific depleted reservoirs for hydrogen storage and highlighted the role of UHS in balancing renewable energy fluctuations. Their work also addressed the challenges of H_2 mixing with residual natural gas and emphasized the importance of proper cushion gas management. Focusing on the critical issue of hydrogen loss, Hagemann et al. [29] conducted laboratory experiments and numerical simulations to investigate hydrogen migration and trapping mechanisms in depleted gas reservoirs. The findings suggested that capillary trapping could significantly reduce hydrogen mobility, potentially improving storage efficiency and security. Regarding practical implementation, Mouli-Castillo et al. [14] conducted a feasibility study for repurposing depleted North Sea gas fields for large-scale H_2 storage. The study highlighted the potential for integrating offshore wind power with UHS to create a sustainable energy system.

Despite these advancements, researchers have observed several natural hazards associated with UHS in depleted reservoirs. These include the potential for H_2 leakage through existing faults, fractures, or poorly sealed wellbores [30], which could lead to environmental contamination or safety [31]. The altered pressure regime within the reservoir after hydrogen injection might also trigger subsidence or induce seismic events, posing a risk to surface infrastructure. Additionally, the interaction between H_2 and residual hydrocarbons or brine in the reservoir could lead to unexpected chemical reactions, potentially compromising the integrity of the storage site [32]. Aluah et al. [33] evaluated the caprock integrity of the Upper Bakken formation which serves as a seal for UHS in the middle Bakken. They concluded that exposure to hydrogen led to increased permeability and porosity over time in reservoir rocks, raising concerns about potential leakage and reduced mechanical stability. Additionally, changes in mineral composition and mechanical properties, including decreased Young's modulus and altered fracture patterns, indicate heightened susceptibility to deformation and leakage risks in the H_2 storage system. Table 4 illustrates the summary of some of the recent work on UHS in depleted gas reservoirs.

Table 4. Summary of recent literature on integrating wind and hydrogen storage in depleted gas fields.

Ref.	Location	Methods	Findings
[34]	Southern North Sea, UK	Well characterization model Chemical stability Leakage assessment	The modeled scenario requires 4–5 GW of power for a six-month injection period, supplying 42% of a natural gas facility's energy capacity and delivering around 100 GWh/day during a 120-day withdrawal period.
[35]	Bohai Bay, China	Mathematical model Economy and environmental compatibility	Wind speed significantly impacts system NPV and LCOH, followed by H_2 prices, with stratum static pressure having the least impact. Annual H_2 production was estimated to be 2.6×10^6 m^3.
[36]	Northern Germany	Experimental studies, reservoir simulation	Salt caverns offer faster cycling capabilities, while depleted gas fields provide larger storage volumes suitable for seasonal energy storage from wind power.
[37]	North Sea, UK	-	Large-scale storage is best suited to porous rock reservoirs. Estimated that 150 TWh of seasonal storage is required to replace seasonal variations in natural gas production.
[38]	North California, USA	Site selection and screening Top sited for H_2 storage Storage and recovery efficiency	Top-ten sites in Northern California have an estimated H_2 storage capacity of 203.5 million tons, making them suitable for seasonal H_2 from renewable energy electrolysis.
[39]	Intermountain west region, USA	Hydrogen storage capacity Site selection Economic analysis	The study reveals that geologic hydrogen storage can provide 72% of the I-WEST region's total energy consumption in 2020. The most cost-effective option is a depleted gas reservoir, with cushion gas type and volume significantly affecting storage costs.
[21]	Southeast and Northeast Brazil	Simulation for site identification Layer approached	Depleted offshore gas fields in Brazil have the potential to store 5483 TWh of H_2, which is equivalent to ten times Brazil's annual electricity consumption.
[40]	Italy	Geological assessment and classification	Identified potential UHS sites, classified based on confidence levels. Existing underground gas stores offer high confidence for hydrogen storage.
[41]	North Sea, Netherlands	Techno-economic analysis, geological assessment	Depleted gas fields could store up to 77 TWh of hydrogen, potentially balancing seasonal wind power fluctuations. Storage is technically feasible and economically viable under certain market conditions

Table 4. *Cont.*

Ref.	Location	Methods	Findings
[42]	North Sea, UK	Geochemical effects study	Assessed fluid-fluid and fluid-rock interactions during UHS, highlighting the need for detailed geochemical analysis
[43]	North California, USA	Geological and reservoir Assessment H_2 production analysis H_2 recovery efficiency evaluation	Northern California's depleted gas fields can store 203.5 million tonnes of H_2 from curtailed renewable energy, with 36% efficiency. Improved recovery and electrolyzer efficiency could enhance this.
[44]	North and Northwest, Poland	Assessment of the size of the pore space of the gas deposit.	Estimates based on the proposed methodology indicate that the average H_2 storage potential for the studied natural gas fields ranges from 0.01 to 42.4 TWh of the H_2 energy equivalent
[45]	Texas, USA	Numerical modeling, sensitivity analysis	Depleted gas reservoirs in Texas could store significant amounts of wind-generated H_2. Reservoir characteristics like porosity and permeability are crucial for determining storage capacity and efficiency.
Present work	Bakken Formation, USA	Mathematical modeling, Simulation	Middle Bakken can storage H_2 54,000, 33,000, 22,000 tons and estimated energy of 1080, 660, and 440 GWh.

3. Study Area

The proposed case study will focus on the Bakken Formation in North Dakota as a potential location for wind H_2 production and underground storage (Figure 4). The Bakken Formation is a geological structure extending across parts of North Dakota, Montana, and Saskatchewan in Canada. Situated at a depth of approximately 3100 m (10,000 feet), it comprises three distinct layers: the Upper, Middle, and Lower Bakken. Recent research has concentrated on the Middle Bakken's geological and petrophysical properties, revealing a porosity range of 3% to 10% and permeability from 0.001 mD to slightly above 0.01 mD [46]. The Upper and Lower Bakken Shale serve as fluid barriers, while the Middle Bakken exhibits varied lithology, including carbonates, sandstones, and fine-grained clastics. The Bakken has yielded over a billion barrels of oil. Currently, there are no specific studies estimating the H_2 storage capacity of Bakken formation. There have been no reports of active faults within the Bakken to disrupt the H_2 storage process. However, since the conditions for CO_2 storage are similar, existing knowledge in that area can be used as a preliminary reference [21,47].

In this study, gamma-ray logs were used to estimate shale volume in a specific zone. Accurate shale volume measurements required data from clean sand and shale rock samples. The Techlog 2024.1 software was employed to estimate shale volume (Vshale) using the gamma-ray method, which utilizes gamma-ray logs as input data to produce the Vshale trace. Total porosity was determined using the neutron density method, which involves neutron porosity logs (NPOR) and bulk density logs (RHOZ) to calculate total porosity (PHIT-ND). Figures 5 and 6 display elevated gamma-ray readings and significant shale volumes in the Upper and Lower Bakken formations across all three wells, indicating the presence of shale rock. Figure 7 illustrates the variable lithology within the Middle Bakken, including sandstone, siltstone, and limestone, consistent with core descriptions. The top and bottom Bakken formations act as barriers, effectively trapping CO_2 in the Middle Bakken. The Bakken Formation is located in the Williston Basin, which is considered a stable intracratonic basin. This geological setting is generally favorable for underground storage operations as it is not near active plate boundaries or major tectonic zones. The Williston Basin contains various structural features, including the Nesson Anticline, Cedar Creek Anticline, and Poplar Dome. These structures are generally considered stable and safe for UHS.

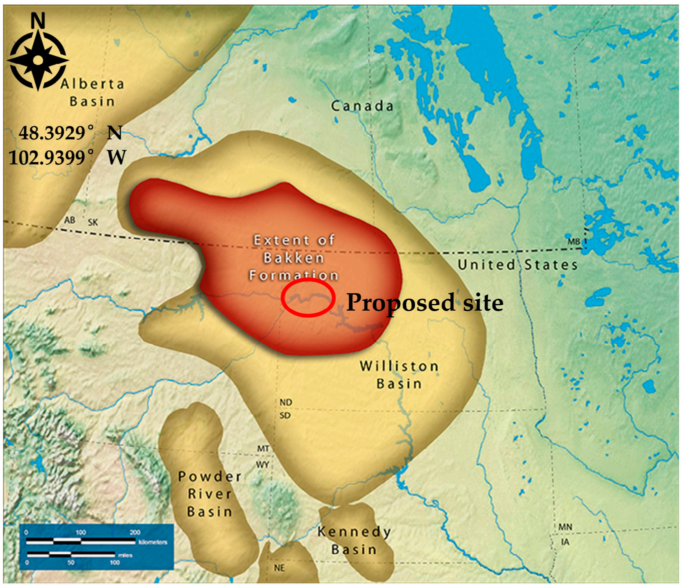

Figure 4. Proposed location.

Historically, the Bakken Formation area has experienced low seismicity. However, there has been an increase in induced seismicity related to oil and gas operations, particularly hydraulic fracturing. These induced seismic events are generally of low magnitude and are considered to pose a low risk for UHS operations in the Bakken Formation.

North Dakota has emerged as a promising state for wind energy production due to its abundant wind resources. Ranking seventh in the nation for wind electricity generation, North Dakota boasts over 4302 MW of installed wind energy capacity, accounting for 36.85% of its net electricity generation [27] and exports approximately 50% of its electricity to neighboring states and Canada. The state's wind power generation capacity has doubled between 2015 and 2021, with more than 2200 wind turbines currently in operation. The largest wind farm, near Williston, has a capacity of 393 MW. North Dakota's annual wind resource is estimated at 1.2 trillion kWh, the highest in the United States. The summary of the wind energy in North Dakota is shown in Table 5.

The integration of wind energy with UHS presents a transformative opportunity to maximize the use of renewable resources and enhance energy sustainability. The Bakken Formation in North Dakota, known for its significant oil and gas reserves, offers a unique potential to repurpose its depleted reservoirs for UHS. This approach not only optimizes the utilization of wind resources but also addresses the intermittency issues associated with wind energy. Despite the state's significant wind resources, there are currently no operational H_2 plants in North Dakota. However, initiatives are underway to develop H_2 production facilities in the state. One notable project is the hydrogen production facility being developed by Bakken Energy's Great Plains Synfuels, which aims to produce up to 380,000 tons of hydrogen per year by 2026. Additionally, the Heartland H_2 hub, spanning several states including North Dakota, Minnesota, Montana, and Wisconsin, has been awarded funding from the U.S. Department of Energy (DOE) under the Biden Infrastructure Job Act (BIJA), with the goal of producing 390,000 tons of H_2 [13]. The potential for North Dakota to become a significant producer of renewable hydrogen is supported by its abundant wind resources, as highlighted in a report by the National Energy Technology Laboratory (NETL) [48].

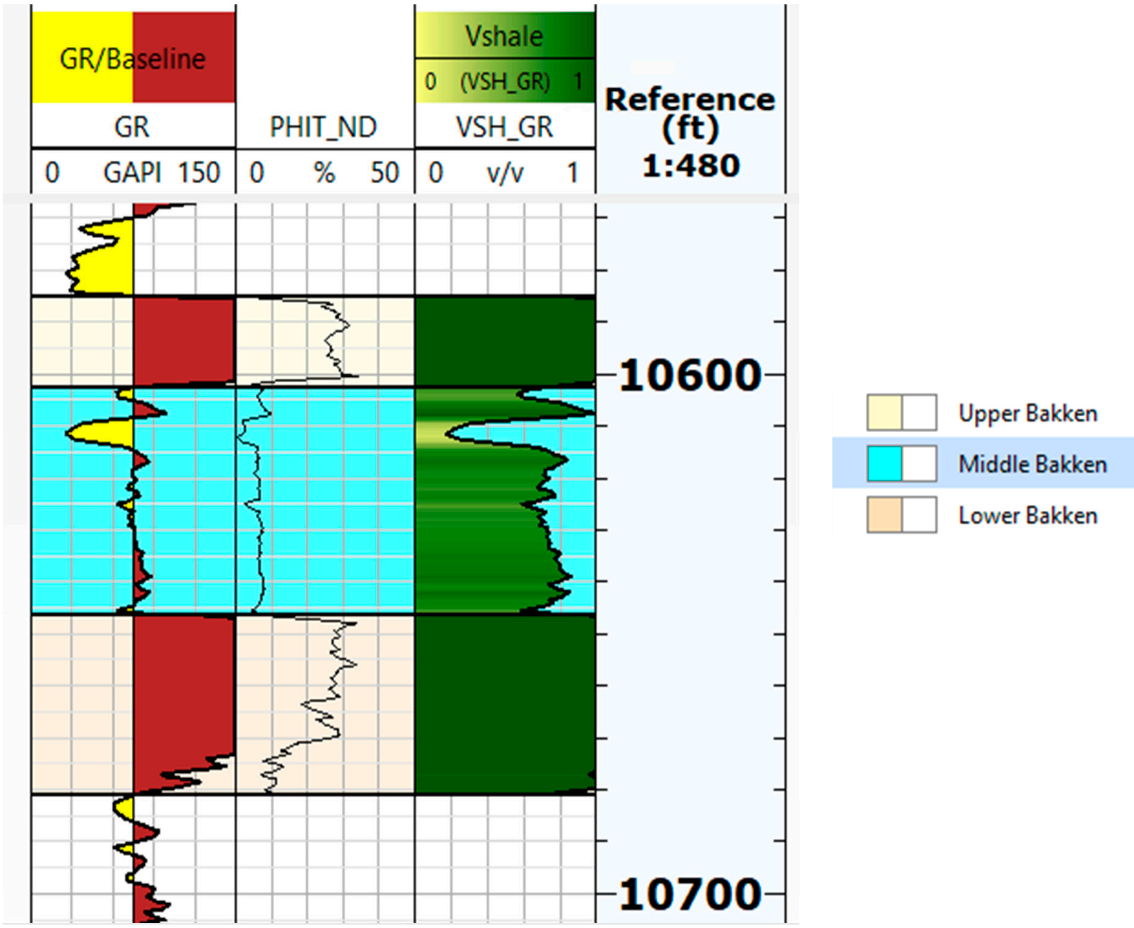

Figure 5. Gamma ray, total porosity, and volume of shale for Bakken formation.

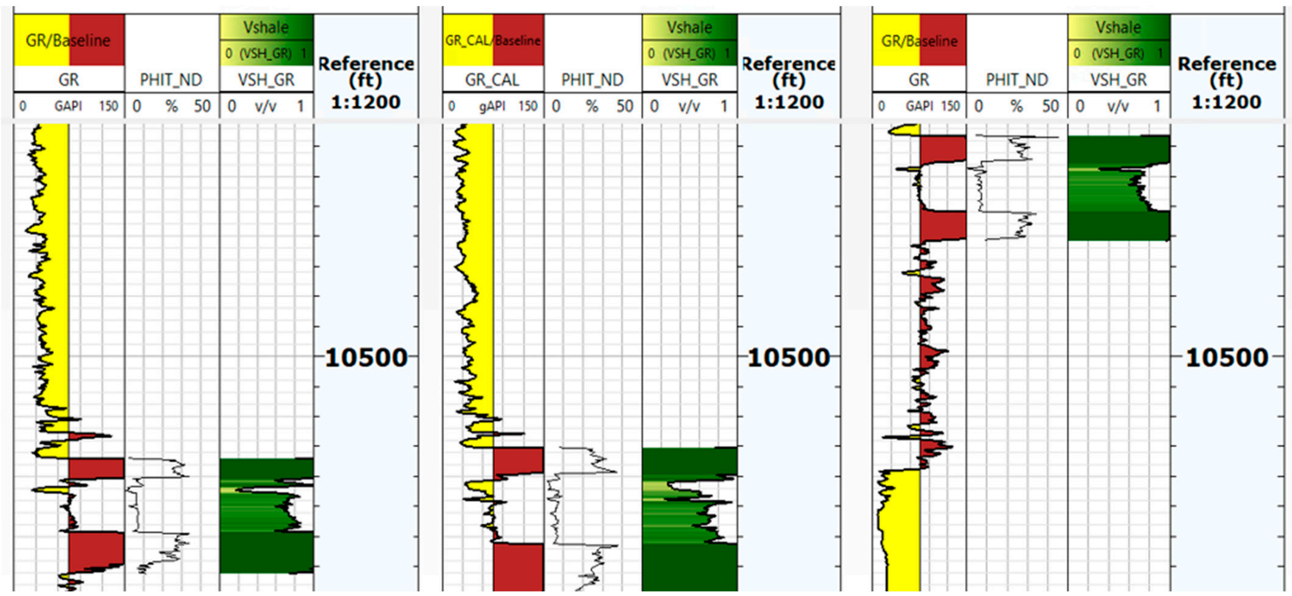

Figure 6. Gamma ray, total porosity, and volume of shale for three wells.

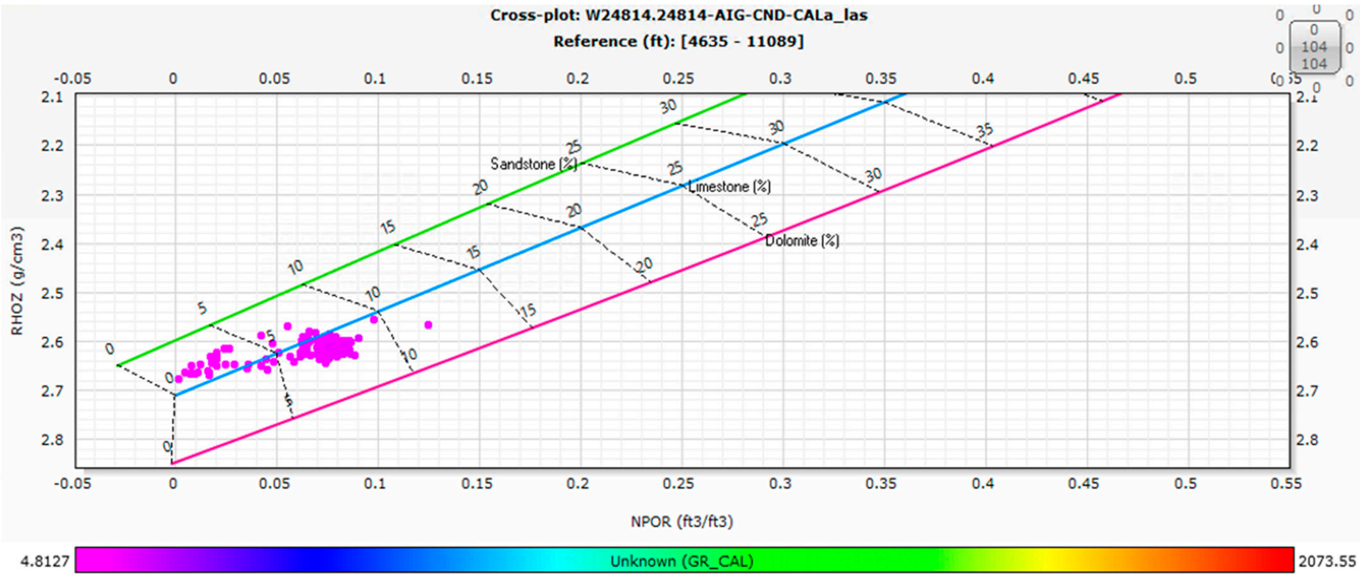

Figure 7. Bulk Density and Neutron Porosity for Well24814.

Table 5. Summary of wind energy in North Dakota.

Potential Wind Capacity	296,084 MW [49]
Current installed wind capacity	4032 MW [27]
Current wind electricity generation	16,571 GWh [27]

4. Methodology

Existing studies and literature under-explore the integration of wind turbines, electrolyzers, and UHS, necessitating further investigation. To assess the performance of such systems, mathematical models are indispensable. Simulation studies employ these models, which are vital for understanding and managing energy and H_2 production in the proposed system. This section first discusses the mathematical models of the system components and presents a strategy for energy management.

4.1. Mathematical Model of the Wind-Electrolyzer-UHS System

A simplified diagram of the proposed system under study is presented in Figure 8. The mathematical representation of all subsystems is presented in brief in the following subsections.

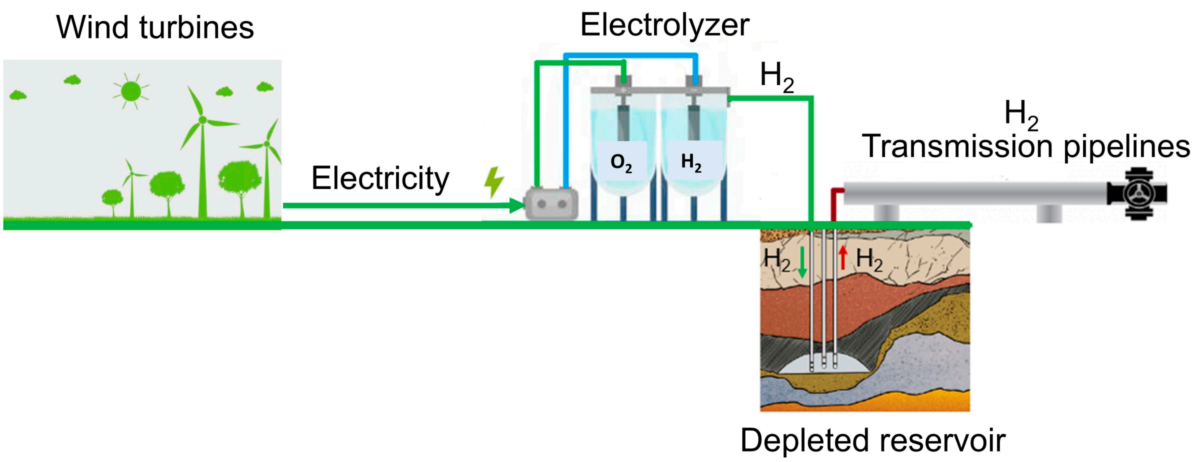

Figure 8. Schematic proposed wind–electrolyzer–underground storage system.

4.1.1. Wind Power System

The power output of a wind turbine can be determined using various methods [49]. In this study, the power curve method is utilized, which assumes a standardized form for the wind turbine's power curve. This curve illustrates the relationship between output power and wind speed at hub height. The power curve, Equation (1), and Equation (2) methods, involve developing characteristic equations to estimate the wind turbine's output across wind speeds ranging from zero to the cut-out speed.

$$P(t) = \begin{cases} 0,\ \mathrm{v} < \mathrm{v_{cutin}} \\ \mathrm{P(v)},\ \mathrm{v_{cutin}} \leq \mathrm{v} < \mathrm{v_{rated}} \\ \mathrm{P_{rated}},\ \mathrm{v_{rated}} \leq \mathrm{v} \leq \mathrm{v_{cutout}} \\ 0,\ \mathrm{v_{cutout}} < \mathrm{v} \end{cases} \tag{1}$$

The power generation function $\mathrm{P(v)}$ is determined using the cubic law which is expressed as:

$$P(\mathrm{v}) = 0.5 \cdot \rho \cdot \mathrm{A} \cdot \mathrm{C_p} \cdot \mathrm{v}^3 \tag{2}$$

In the Equations, the variables are defined as follows: $\mathrm{v_{cutin}}$ denotes the cut-in speed, $\mathrm{v_{rated}}$ represents the rated speed, and $\mathrm{v_{cutout}}$ indicates the cut-out speed.

In Equation (2), ρ represents the air density, A indicates the rotor swept area, and $\mathrm{C_p}$ represents the power coefficient. To simplify the calculations, a maximum achievable $\mathrm{C_p}$ value of 0.4 is assumed. Equation (3) is used to ascertain the wind farm's overall time-varying effect, taking into account the number of wind turbines in the farm, denoted by n.

$$\mathrm{P_{total\ wind}(t)} = \sum_{i=1}^{n} P_n(t) \tag{3}$$

4.1.2. Hydrogen Production Using Wind Energy

Although the wind farm is specifically designed for hydrogen production, it must also provide all the electricity needed for ancillary services like water filtration/desalination and H_2 compression. This study utilized the PEM electrolyzer model introduced by Dinh et al. [50]. Equation (4) is used to calculate the theoretical quantity of H_2 that can be generated per hour, based on the wind farm's output to determine the theoretical amount of H_2 which can be produced each hour based on the output of the wind farm.

$$\mathrm{m_{H_{2,theory}}(t)} = \frac{\mathrm{P_{wind}(t)}}{\frac{\mathrm{E_{elec}}}{\eta_{\mathrm{conv}}} + \mathrm{E_{pcl}}} [\mathrm{kg/h}] \tag{4}$$

where $\mathrm{E_{elec}}$ represents the electricity consumption specified by the electrolyzer manufacturer the manufacturer of the electrolyzers. $\mathrm{E_{pcl}}$ represents the electricity required for other components associated with the electrolyzer, including water purification, other losses. η_{conv} represents the conversion efficiency.

Equation (5) mathematically represents the practical hourly production of H_2.

$$\mathrm{m_{H_{2,practical}}(t)} = \frac{\mathrm{P_{H2plant}} \cdot \eta_{\mathrm{conv}}}{\mathrm{E_{elec}}} [\mathrm{kg/h}] \tag{5}$$

where, $\mathrm{P_{H2plant}}$ is called the rated capacity of H_2 electrolyzer and should be.

$$\mathrm{P_{H2plant}} \leq max\ \mathrm{m_{H_{2,theory}}(t)}\ \mathrm{E_{elec}}\ [\mathrm{MW}] \tag{6}$$

In order to correctly quantify the H_2 production per hour, this study also incorporated three conditions as defined in Dinh et al. [50]. These conditions are low wind power, wind power capable of operating the H_2 plant at its nominal capacity, and wind power below the nominal capacity ($P_{H2plant}$). To ensure an efficient operation, the electrolyzers should be shut down when the input power (i.e., the real-time output from the wind farm) falls below a certain threshold. This lower limit, Pfarm_low, is set at 5% of the electrolysis plant's rated capacity, as indicated in Equation (7).

$$P_{wind,min} = 0.05 \cdot P_{H2plant} \quad (7)$$

A series of characteristic equations in Equation (8) were formulated to measure the H_2 production, taking into account the electrolyzer's nominal capacity and the power produced by the wind farm.

$$m_{H_{2,practical}}(t) = \begin{cases} 0, \ P_{wind}(t) \leq P_{wind,min} \\ \frac{P_{wind}(t)}{\frac{E_{elec}}{\eta_{conv}} + E_{pcl}}, \ P_{wind}(t) < P_{H2plant} \\ \frac{P_{H2plant} \cdot \eta_{conv}}{E_{elec}}, \ P_{wind}(t) \geq P_{H2plant} \end{cases} \quad (8)$$

4.1.3. North Dakota Depleted Oil and Gas Fields Storage Capacity in the Antelope Field

Well data from North Dakota Industrial Commission such as depth to top of formation, porosity and thickness were utilized for final calculations of capacity estimates. Formation tops were correlated from well logs whereas porosity values were assigned from log curves and quality control (QC) techniques with core data.

H_2 storage in the antelope field (Approximately 46,000 acres) was estimated using two approaches: pore volume per acre approach and storativity approach.

Pore Volume Per Acre Approach

The pore volume per acre approach can be used to estimate reserves by finding the pore space within the formation on a per acre basis. This approach is commonly utilized in the oil and gas sector for an initial approximation of reserves.

$$\text{Pore volume} = \text{A h } \phi \quad (9)$$

where A is area (acres), h is thickness (ft), ϕ is the porosity (fraction).

Storativity Approach

The Storativity approach is a reservoir engineering tool used to assess the storage capacity of subsurface reservoirs. It is used to measure the ability of a reservoir to store fluids such as oil, gas, and water.

$$\text{Storativity} = \frac{\sum \varnothing \cdot h}{\text{cum}(\varnothing \cdot h)} \quad (10)$$

where h is thickness (ft), ϕ is the porosity (fraction)

Storage capacity estimate for antelope study area is mathematically represented as.

$$G_{H2} = \frac{PV \cdot \rho_{H2} \cdot E}{1000\left(\frac{\text{kg}}{\text{tones}}\right)} \quad (11)$$

where, G_{H2} is the total mass of H_2 could be potentially stored (tons). PV, ρ_{H2}, and E are total effective pore space in m^3, density of H_2 under reservoir temperature and pressure in kg/m^3, and storage capacity coefficient, respectively.

4.2. Energy and Hydrogen Production Strategy

Figure 9 illustrates the general control system employed for power and H_2 production. The electrolyzer is only activated when the wind power reaches or surpasses 5% of the electrolyzer's rated capacity. Conversely, if the wind power falls below this threshold, the electrolyzer is deactivated to prevent unnecessary toggling. Consequently, H_2 production remains minimal during this low power range. In the case where the wind turbine's power output hits this minimum threshold, two scenarios arise. The first scenario involves the continuous operation of the control system, wherein all the wind power is utilized for H_2 production. When wind power is greater than the maximum electrolyzer capacity, H_2 is produced at maximum electrolyzer capacity and excess power gets curtailed, which will be discussed in future work.

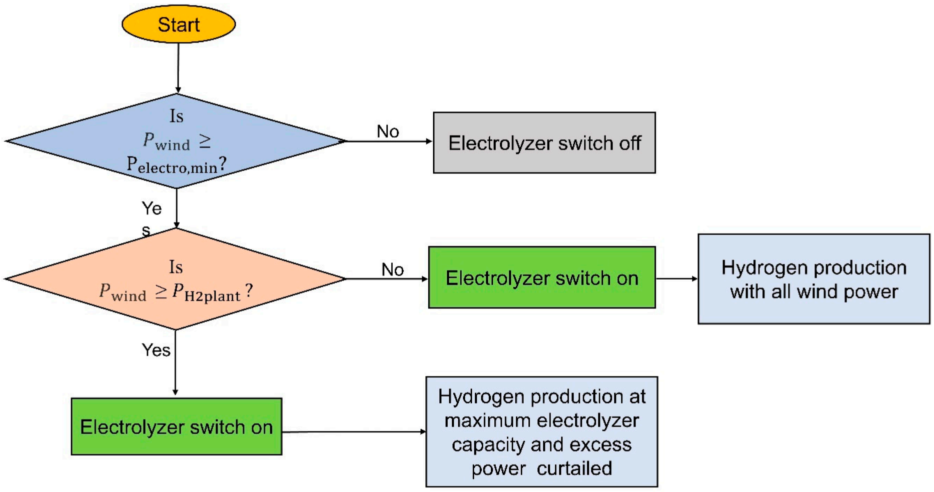

Figure 9. Overview of the control system.

5. Assumptions and System Parameters

5.1. Assumptions

The wind and electrolyzer data, the reservoir characterization and selection process, and the mathematical modeling assumptions and parameters used to simulate wind, H_2 production, and storage systems may all contain some degree of uncertainty or error.

To deal with utility-scale wind farms containing multiple wind turbines, the study utilized aggregated modeling techniques. This approach aims to represent the whole farm as a single equivalent unit with a re-scaled power capacity, which simplifies the system's complexity and reduces computation time significantly.

This study does not include cost and market analyses, plant siting, or sizing.

It is assumed that all the wind resources that are available are harnessed.

There are numerous H_2 storage options available, but only underground storage in depleted oil and gas fields is considered in this study.

The study did not consider the reactions between H_2 and the subsurface rock and fluid, geo-mechanical effects, or microbial activity.

The amount of water required for the study was not included.

Additionally, the findings might only apply directly to the unique geological and environmental conditions of North Dakota's Bakken Formation, not to other regions or formations.

5.2. Wind Data

The General Electric model, with a nominal capacity of 1.5 MW, is the chosen wind turbine for the proposed wind farm. Table 6 provides detailed specifications of the wind turbine. The wind data used for the analysis was retrieved from the North Dakota Agricultural Weather Network (NDAWN) at a height of 10 m [51]. However, we reanalyzed these data using the vertical wind profile equation to estimate wind conditions at a height of 80 m. Figure 10 provides a visual representation of this reanalyzed wind data. The minimum value of the wind speed should be 3.5 m/s for the process to be realized.

Table 6. Turbine specifications used in the case study [52].

Parameters	Value
rated power	1.5 MW
cut-in wind speed	3.5 to 4 m/s
cut-out wind speed	20 to 25 m/s
rotor diameter	77 m
hub heights	80 m
rated wind speed	11.2 m/s
air density	1.225 kg/m^3
power coefficient	0.4

Mathematically, the process of reanalyzing wind data from 10 m to 80 m can be expressed as follows:

$$V_{80} = V_{10}\left(\frac{H_{80}}{H_{10}}\right)^{\alpha} \quad (12)$$

where V_{80} and V_{10} are the wind speeds at height H_{80} and H_{10} and α is the wind shear exponent and considered value is 0.2.

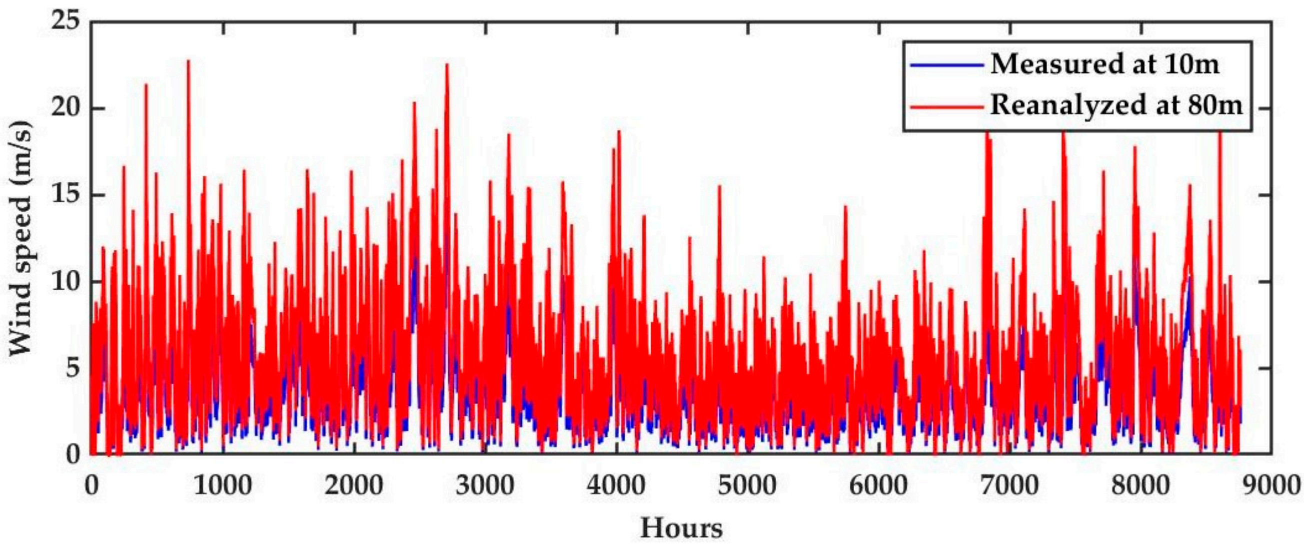

Figure 10. Wind profile in Williston (collected from: North Dakota Agricultural Weather Network [51]).

5.3. Electrolyzer Data

The technology chosen for this study is the Proton exchange membrane electrolyzer. In this research, it is assumed that the electrolyzers will operate exclusively based on the variable power produced by the wind farm, with no grid support. The parameters for the electrolyzer, sourced from Dinh et al. [50], are detailed in Table 7. Consequently, the electrolyzers function intermittently, aligning with the fluctuating wind power input.

Table 7. Parameters for electrolyzer.

Parameters	Value
Energy used for electrolysis E_{elec}	50 kWh/kg [53]
Water purification energy, H_2 losses and compression, E_{pcl}	3 kWh/kg
Conversion efficiency η_{conv}	90%
Plant size $P_{H2plant}$	13 MW
Stack lifetime	12.5 years

5.4. Reservoir Data

The storage potential of the depleted oil and gas field was assessed using well data provided by the North Dakota Department of Mineral Resources (NDDMR). The available log data for the field, detailed in Table 8, was imported into Techlog, a petrophysical analysis and data visualization software developed by Schlumberger. This log data were utilized to measure the reservoir's average porosity, net-to-gross ratio, and both gross and net thickness.

Table 8. Reservoir parameters for three wells [54].

Well Middle Bakken	Top (ft)	Bottom (ft)	Gross (ft)	Net (ft)	Net to Gross	Average Porosity (%)
W24814	10,603.3	10,655.06	51.75	9.5	0.184	2.7
W19693	10,602.63	10,646.18	43.55	5	0.115	2.0
W26990	10,342.7	10,378.22	35.52	1.5	0.042	1.6

Two different approaches, outlined in Equations (9) and (10), were used to estimate the H_2 storage capacity of the antelope field (Table 9). Both approaches were used to ensure consistency and validation of the results obtained from each method. Figure 11 illustrates the proportional correlation between storativity and depth for three wells.

Table 9. Pore Volume Per Acre and storativity for three wells.

Well (Middle Bakken)	Pore Volume Per Acre (ft)	Storativity Cum. Por-Th (ft)
W24814	60,864.21	329.04
W19693	37,938.15	252.29
W26990	24,756.02	237.09

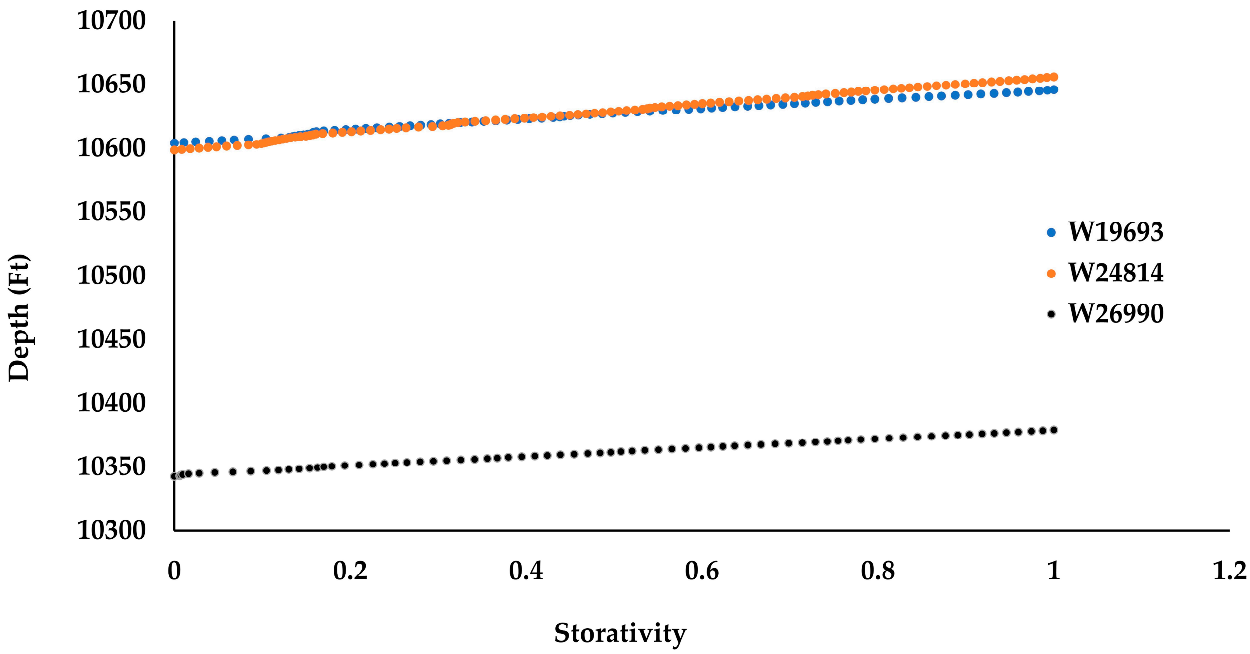

Figure 11. Storage capacity for Well W19693, W24814 and W26990.

6. Results

6.1. Quantifying Storage Capacity in the Antelope Field

The well (W24814) demonstrated the best storage capacity using the previous two methods, Equations (9) and (10), and had the optimal volume for potentially storing large quantities of hydrogen. Consequently, well W24814 was chosen for the case study. Each well in the Middle Bakken formation was evaluated using low, mid, and high scenarios. A 5% allowance was applied to two key reservoir parameters—gross thickness and porosity—since these significantly influence reserve estimation. This 5% allowance was used to estimate the storage capacity based on the pore volume as described in Equation (11). A conservative value of 0.04 for E was used in our study, considering H_2′s density under reservoir temperature and pressure, as well as reservoir properties. The summary of pore volume and storage capacity for the selected Middle Bakken wells is presented in Table 10.

Table 10. Pore volume and store capacity for the selected Middle Bakken wells.

Middle Bakken Formation	Pore Volume (10^6 m^3)			H_2 Capacity (10^6 Tonnes)		
	Low	**Mid**	**High**	**Low**	**Mid**	**High**
W24814	71.550	79.280	87.406	0.048	0.054	0.059
W19693	44.602	49.421	54.486	0.030	0.033	0.037
W26990	29.103	32.247	35.552	0.020	0.022	0.24

Core and log data from the Antelope field were utilized for calibration in this study (Figures 12–14). Given the limited core data for most formation depths, porosity cross-plots were generated using the available core depths. These cross-plots were essential in refining the data, removing anomalies, and enhancing correlation coefficients. The findings show that the porosity values obtained from well logs were highly representative, resulting in accurate reserve estimates.

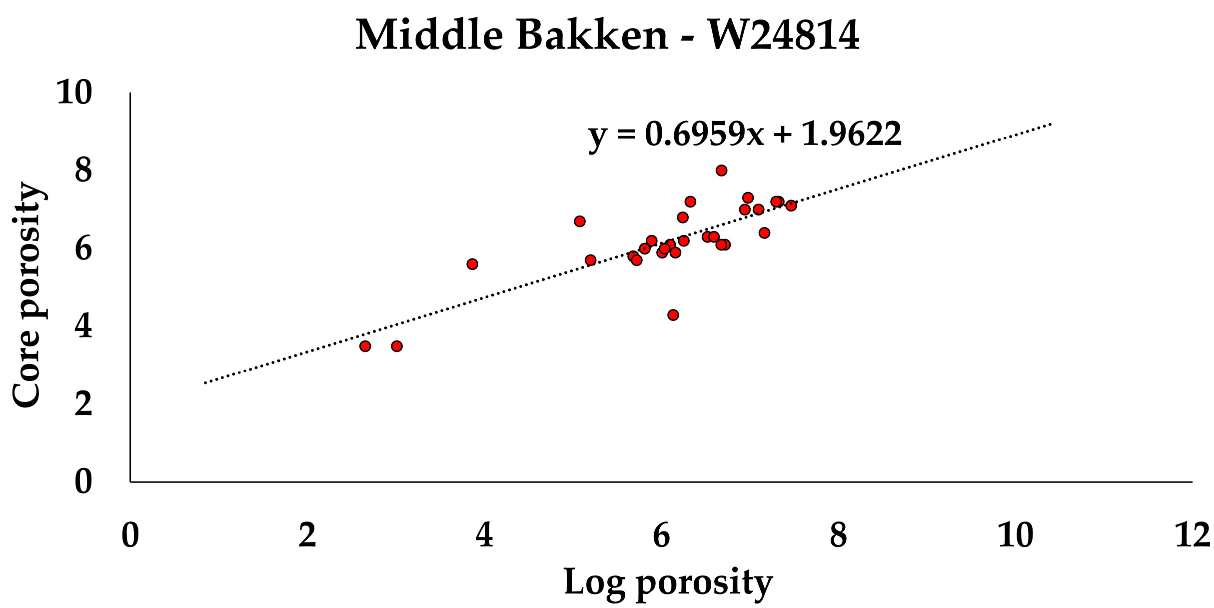

Figure 12. Porosity cross-plots for W24814.

In this study, the primary focus was on estimating storage capacity using pore volume, a standard method in the industry for preliminary assessments, without considering wellbore integrity or potential leakage. To enhance the accuracy of the evaluation, the authors also incorporated a core analysis and log analysis, which provided detailed insights into the reservoir's properties. These methods enable a better understanding of the formation's porosity, permeability, and other critical factors that influence H_2 storage potential. While the initial assessment is based on pore volume, core and log analyses help refine the understanding of the reservoir's suitability for H_2 storage. Future work with wellbore integrity and potential leakage can utilize the modeling approach for a more thorough evaluation.

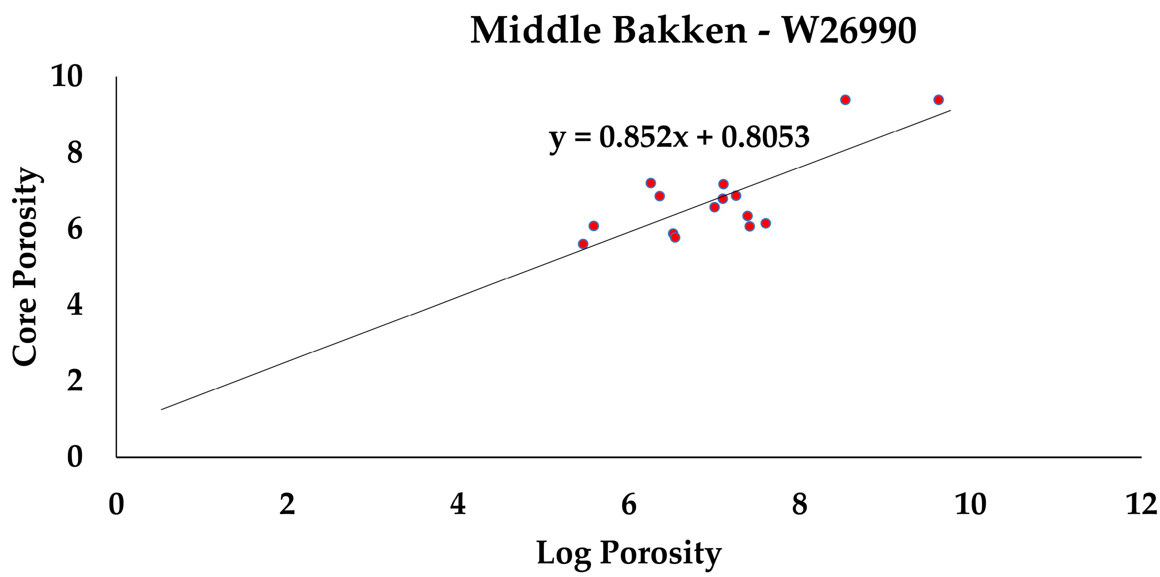

Figure 13. Porosity cross-plots for W26990.

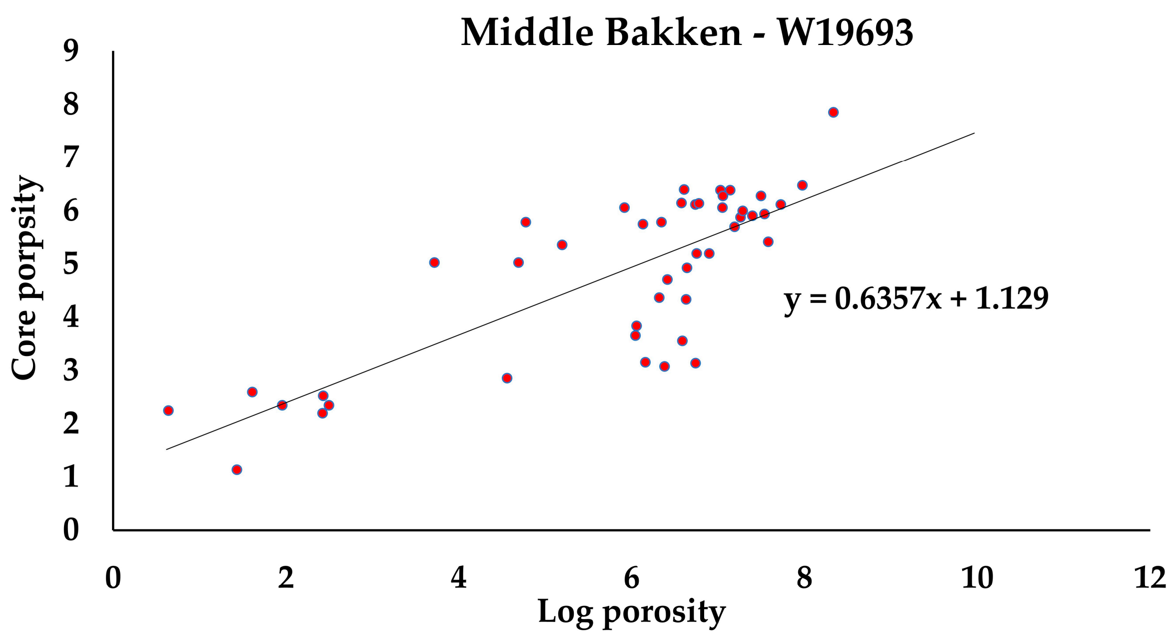

Figure 14. Porosity cross-plots for W19693.

6.2. Energy and Hydrogen Production Simulation

In this operation, the wind farm generates electricity as usual, supplying electricity to the electrolyzer for H_2 production without any grid support. As a result, the electrolyzers operate intermittently, depending on the fluctuating power input. The installed capacity is 15 MW, with each unit having a capacity of 1.5 MW, giving a scale factor of 10. Wind power production fluctuates throughout the year, as shown in the hourly wind profile (Figure 15). The simulation was run using average hourly wind data for one year, from 1 January 2023 to 31 December 2023. For simplicity, the data were averaged for each hour over the period from 1 January 2023 to 31 January 2023, for the Middle Bakken. The simulation results in Figure 15 indicate that the annual average power output from the wind farm and the hydrogen production exhibit similar patterns and align well. This alignment confirms that the model accurately calculates both H_2 production and average power outputs. The correlation between the hourly power output and H_2 production in Figure 15 further validates the model's effectiveness.

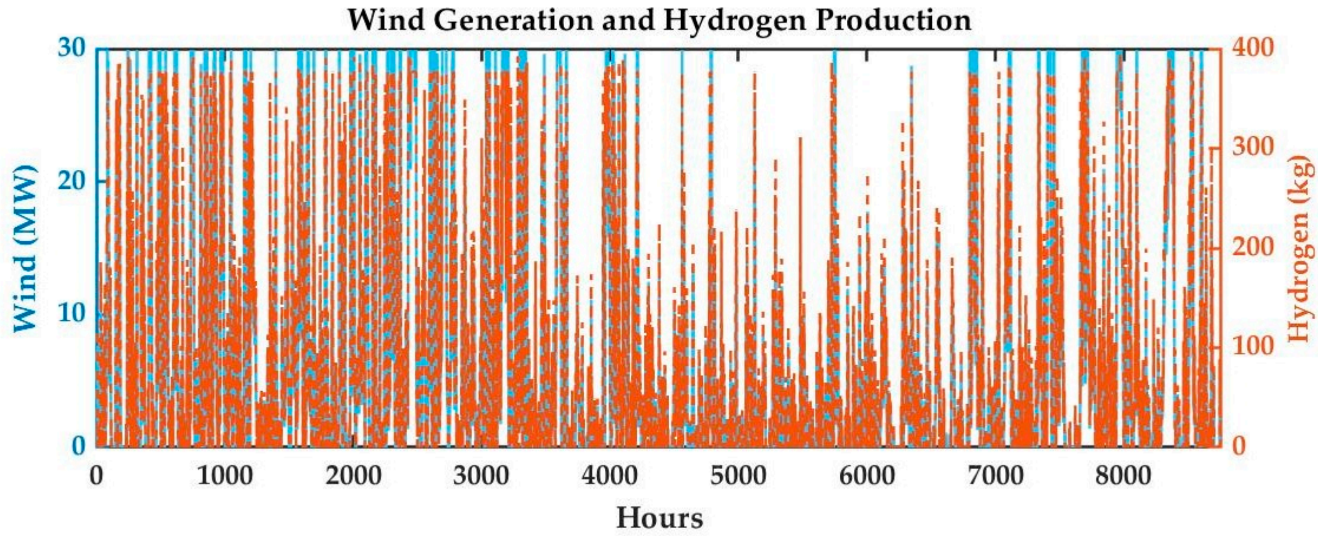

Figure 15. Hourly power output from the wind farm and hydrogen production.

These results (Figure 16) show a total production of 386,370 kg of H_2 from a 15 MW wind farm, which can be stored for at least 140 days in the depleted reservoir (W24814) with a capacity of 54,000 tons, which is equivalent to 1080 GWh of energy using 60% system efficiency. During this period, the wind farm generated 27.039 GWh, with 1.936 GWh curtailed due to the electrolyzer's capacity limitations. Similarly, for wells W19693 and W26990, H_2 can be stored for at least 86 days and 57 days, with energy storage of 660 and 440 GWh, respectively, using the same wind profile.

Table 11 emphasizes the seasonal H_2 production and storage during the four seasons namely winter, spring, summer, and fall. During the summer, the wind speed is low compared to other seasons while spring has the highest wind speed in the Bakken region. As a result, the summer season requires more days to store H_2, whilst the spring season requires the least number of days.

In the field of geological H_2 storage, various geological factors significantly influence storage capacity and efficiency. Heinemann et al. [36] explored the impact of porosity and permeability on H_2 storage within porous media. Their study concluded that higher porosity and permeability generally enhance storage capacity and injectivity; however, they cautioned that excessive permeability could lead to H_2 migration, underscoring the necessity of proper caprock sealing. A high intrinsic permeability is required to ensure well deliverability, with a minimum value of 50md and an effective porosity of greater than 10% for sandstones [55]. The study observed varying storage capacities across different wells (W24814, W19693, and W26990), which can be attributed to differences in porosity and permeability, in line with Heinemann et al. [36]'s findings. Additionally, Flesch et al. [56] investigated the geochemical interactions between H_2 and caprock minerals, emphasizing the crucial role of caprock integrity in preventing H_2 leakage and ensuring long-term storage stability. Although the study did not directly assess caprock integrity, the successful storage durations (140, 86, and 57 days for the respective wells) indicate sufficient sealing properties within the Bakken formation. Moreover, Amid et al. [34] examined the effects of reservoir pressure and temperature on H_2 storage capacity in depleted gas fields. They found that higher pressures generally enhance storage capacity, while temperature effects are more complex. The differences in storage capacities across the wells in the study, reflecting variations in pressure and temperature conditions within the Bakken formation, are consistent with Amid et al. [34]'s findings.

Table 11. Seasonal wind and H_2 production.

Season	Wind Power (GWh)	Hydrogen Production (kg)	Reservoirs Storage in Days		
			W24814	W19693	W26990
Winter (December 1 to February 28)	73.86	106,350	508	310	207
Spring (March 1 to May 31)	98.63	138,590	390	239	159
Summer (June 1 to August 31)	40.5	58,980	916	560	373
Fall (September 1 to Novemebr 31)	57.33	82,449	655	401	267

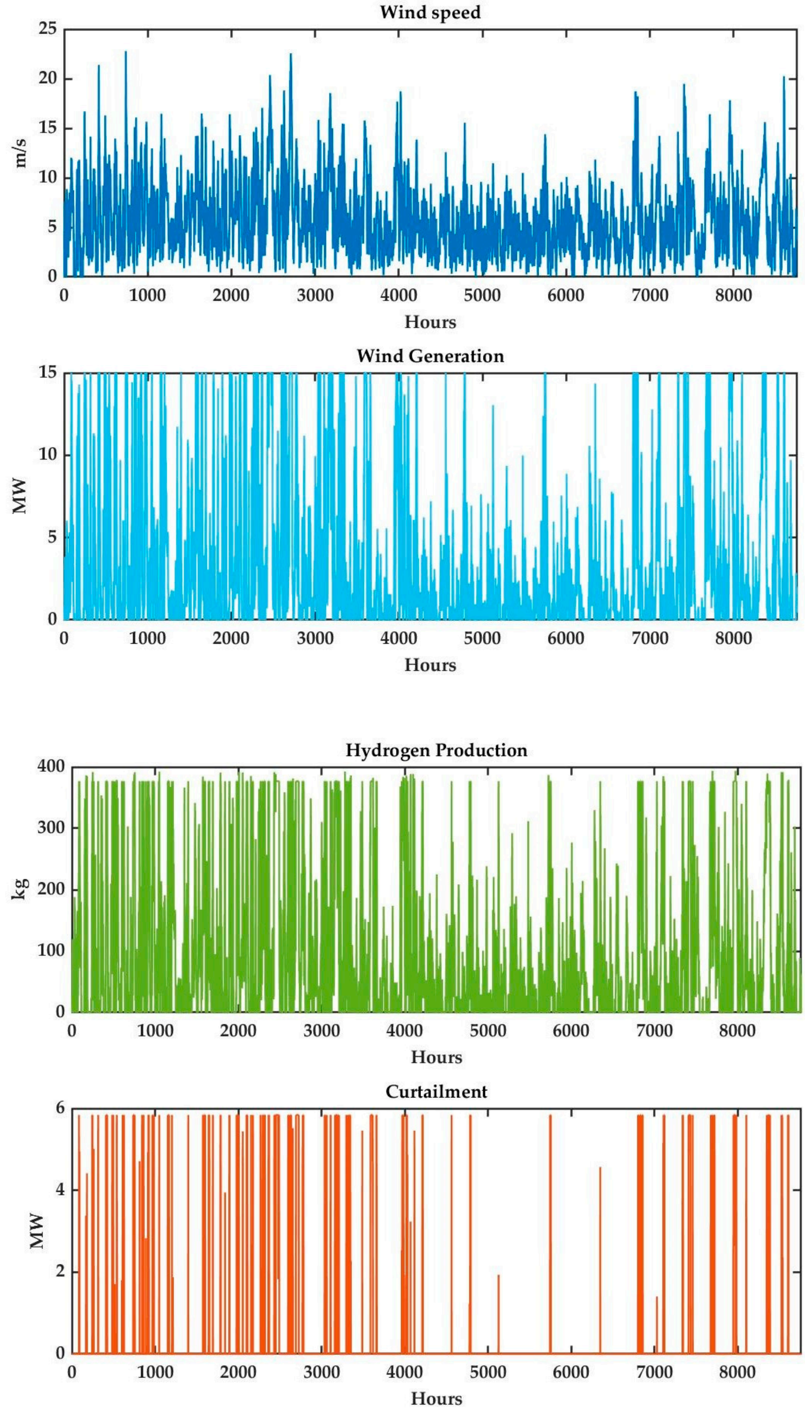

Figure 16. Annual wind speed, power generation, hydrogen production and power curtailment for W24814.

7. Conclusions and Recommendations

This research introduces a novel co-located system approach to energy storage by integrating wind power with UHS within the depleted oil and gas reservoirs of the Bakken Formation, North Dakota. The study's key innovation lies in repurposing a region historically associated with fossil fuels for sustainable energy storage, thereby addressing the intermittency of wind sources. The focus areas of this research are: (i) determining total reservoir capacity; (ii) evaluating H_2 production; and (iii) calculating the minimum amount of time in days that it takes to store the produced hydrogen. The analysis revealed that the selected wells, i.e., W24814, W19693, and W26990 in the Middle Bakken Formation have significant storage capacities of 54,000, 33,000, and 22,000 tons, with potential storage durations ranging from 57 to 140 days, depending on the well. By combining weather data with mathematical models, available wind power and H_2 production were estimated. These results not only validate the feasibility of large-scale H_2 storage in the Bakken Formation but also highlight its potential to enhance the reliability of wind energy systems.

In terms of future research directions, the authors recommend conducting experiments and real-time simulations to explore the hydrodynamics, geochemical aspects, and microbial factors that influence storage capacity, gas containment efficiency, and withdrawal processes. Accurately modeling the behavior of such plants will provide valuable insights for controlling and operating future H_2 storage systems. Therefore, future work should incorporate wellbore integrity and potential leakage for a more comprehensive assessment. Furthermore, they suggest upgrading the model to incorporate a techno-economic framework and dynamic modeling. The study is expected to assist researchers in conducting scenario analyses, validating theoretical findings, and optimizing system operation in future investigations, further solidifying the role of geological H_2 storage in the global energy transition.

Author Contributions: Conceptualization, writing—original draft preparation, S.O.B. and E.G; writing—review and editing, S.O.B., O.S.T., E.G., R.A., R.J. and T.O.; supervision, O.S.T. All authors have read and agreed to the published version of the manuscript.

Funding: This research received no external funding.

Data Availability Statement: All data are available on request from the corresponding author.

Acknowledgments: The authors gratefully acknowledge the Department of Energy Engineering and Department of Petroleum Engineering, University of North Dakota, for motivating us to publish this paper.

Conflicts of Interest: The afore-mentioned authors declare no conflicts of interest.

Nomenclature

BIJA	Biden Infrastructure Job Act
Cp	Power coefficient
DOE	Department of Energy
E_{elec}	Electricity consumption
EERC	Energy and Environmental Research Center
GE	Generic Electric
GHG	Greenhouse gas
GWh	Giga watt hour
mD	Milli diameter
MW	Megawatt
NDAWN	North Dakota Agricultural Weather Network
NDDMR	North Dakota Department of Minerals Resources
NETL	National Energy Technology Laboratory
NREL	National Renewable Energy Laboratory
PEM	Proton exchange membrane
SMR	Steam methane reforming

UHS	Underground hydrogen storage
V_{cutin}	Cut in speed
V_{cutout}	Cut out speed
ϕ	Porosity fraction
η_{conv}	Conversion efficiency

References

1. Muhammed, N.S.; Haq, B.; Shehri, D.A.; Al-Ahmed, A.; Rahman, M.M.; Zaman, E.; Iglauer, S. Hydrogen storage in depleted gas reservoirs: A comprehensive review. *Fuel* **2023**, *337*, 127032. [CrossRef]
2. Bade, S.O.; Meenakshisundaram, A.; Omojiba, T.; Tomomewo, O. Battery Uses for Regulating Active Power in Utility-scale Wind-based Hybrid Power Plant. *Am. J. Energy Res.* **2023**, *11*, 82–92. [CrossRef]
3. Raad, S.M.J.; Leonenko, Y.; Hassanzadeh, H. Hydrogen storage in saline aquifers: Opportunities and challenges. *Renew. Sustain. Energy Rev.* **2022**, *168*, 112846. [CrossRef]
4. Bade, S.O.; Tomomewo, O.; Meenakshisundaram, A. Utility-Scale Wind-Based Hybrid Power Plants and Control Strategy. *Sustain. Energy* **2023**, *11*, 12–20. [CrossRef]
5. Abe, J.; Popoola, A.; Ajenifuja, E.; Popoola, O. Hydrogen energy, economy and storage: Review and recommendation. *Int. J. Hydrogen Energy* **2019**, *44*, 15072–15086. [CrossRef]
6. Gatto, A.; Sadik-Zada, E.R.; Lohoff, T.; Aldieri, L.; Vinci, C.P.; Peitz, K.A. An exemplary subsidization path for the green H_2 economy uptake: Rollout policies in the US and the European Union. *J. Clean. Prod.* **2024**, *440*, 140757. [CrossRef]
7. Nasiritousi, N.; Grimm, J. Governing toward decarbonization: The legitimacy of national orchestration. *Environ. Policy Gov.* **2022**, *32*, 411–425. [CrossRef]
8. Gulli, C.; Heid, B.; Noffsinger, J.; Waardenburg, M.; Wilthane, M. *Global Energy Perspectives 2023: Hydrogen Outlook*; McKinsey & Company: Chicago, IL, USA, 2024.
9. Ndulue, U.F.; Tomomewo, O.S.; Khalifa, H. A Comprehensive Review of Fishbone Well Applications in Conventional and Renewable Energy Systems in the Path towards Net Zero. *Fuels* **2023**, *4*, 376–396. [CrossRef]
10. Ikuerowo, T.; Bade, S.O.; Akinmoladun, A.; Oni, B.A. The integration of wind and solar power to water electrolyzer for green hydrogen production. *Int. J. Hydrogen Energy* **2024**, *76*, 75–96. [CrossRef]
11. Bade, S.O.; Tomomewo, O.S.; Meenakshisundaram, A.; Ferron, P.; Oni, B.A. Economic, social, and regulatory challenges of green hydrogen production and utilization in the US: A review. *Int. J. Hydrogen Energy* **2023**, *49*, 314–335. [CrossRef]
12. Hassan, Q.; Abbas, M.K.; Tabar, V.S.; Tohidi, S.; Abdulrahman, I.S.; Salman, H.M. Sizing electrolyzer capacity in conjunction with an off-grid photovoltaic system for the highest hydrogen production. *Energy Harvest. Syst.* **2023**, *10*, 331–348. [CrossRef]
13. Bade, S.O.; Tomomewo, O.S. A review of governance strategies, policy measures, and regulatory framework for hydrogen energy in the United States. *Int. J. Hydrogen Energy* **2024**, *78*, 1363–1381. [CrossRef]
14. Mouli-Castillo, J.; Heinemann, N.; Edlmann, K. Mapping geological hydrogen storage capacity and regional heating demands: An applied UK case study. *Appl. Energy* **2021**, *283*, 116348. [CrossRef]
15. Chen, Y.; Jin, X.; Zeng, L.; Zhong, Z.; Mehana, M.; Xiao, W.; Pu, W.; Regenauer-Lieb, K.; Xie, Q. Role of large-scale underground hydrogen storage and its pathways to achieve net-zero in China. *J. Energy Storage* **2023**, *72*, 108448. [CrossRef]
16. Sambo, C.; Dudun, A.; Samuel, S.A.; Esenenjor, P.; Muhammed, N.S.; Haq, B. A review on worldwide underground hydrogen storage operating and potential fields. *Int. J. Hydrogen Energy* **2022**, *47*, 22840–22880. [CrossRef]
17. Zivar, D.; Kumar, S.; Foroozesh, J. Underground hydrogen storage: A comprehensive review. *Int. J. Hydrogen Energy* **2021**, *46*, 23436–23462. [CrossRef]
18. Andersson, J.; Grönkvist, S. Large-scale storage of hydrogen. *Int. J. Hydrogen Energy* **2019**, *44*, 11901–11919. [CrossRef]
19. Matos, C.R.; Carneiro, J.F.; Silva, P.P. Overview of Large-Scale Underground Energy Storage Technologies for Integration of Renewable Energies and Criteria for Reservoir Identification. *J. Energy Storage* **2019**, *21*, 241–258. [CrossRef]
20. Bade, S.O.; Taiwo, K.; Ndulue, U.F.; Tomomewo, O.S.; Oni, B.A. A review of underground hydrogen storage systems: Current status, modeling approaches, challenges, and future prospective. *J. Hydrogen Energy* **2024**, *80*, 449–474. [CrossRef]
21. Ciotta, M.; Tassinari, C.; Zacharias, L.G.L.; Van Der Zwaan, B.; Peyerl, D. Hydrogen storage in depleted offshore gas fields in Brazil: Potential and implications for energy security. *Int. J. Hydrogen Energy* **2023**, *48*, 39967–39980. [CrossRef]
22. U.S. Department of Energy. U.S. National Clean Hydrogen Strategy and Roadmap. 2023. Available online: https://www.hydrogen.energy.gov/docs/hydrogenprogramlibraries/pdfs/clean-hydrogen-strategy-roadmap.pdf?Status=Master (accessed on 30 June 2024).
23. Lord, A.S.; Kobos, P.H.; Borns, D.J. Geologic storage of hydrogen: Scaling up to meet city transportation demands. *Int. J. Hydrogen Energy* **2014**, *39*, 15570–15582. [CrossRef]
24. Tarkowski, R. Underground hydrogen storage: Characteristics and prospects. *Renew. Sustain. Energy Rev.* **2019**, *105*, 86–94. [CrossRef]
25. Epelle, E.I.; Obande, W.; Udourioh, G.A.; Afolabi, I.C.; Desongu, K.S.; Orivri, U.; Gunes, B.; Okolie, J.A. Perspectives and prospects of underground hydrogen storage and natural hydrogen. *Sustain. Energy Fuels* **2022**, *6*, 3324–3343. [CrossRef]
26. North Dakota Labor Market Information. North Dakota Oil and Gas Economy. 2023. Available online: https://ndlegis.gov/files/committees/65-2017/19_5029_03000appendixj.pdf (accessed on 6 May 2024).

27. Energy Information Administration. North Dakota State Profile and Energy Estimates. 2022. Available online: https://www.eia.gov/state/?sid=ND (accessed on 23 May 2024).
28. Tarkowski, R.; Uliasz-Misiak, B. Towards underground hydrogen storage: A review of barriers. *Renew. Sustain. Energy Rev.* **2022**, *162*, 112451. [CrossRef]
29. Hagemann, B.; Rasoulzadeh, M.; Panfilov, M.; Ganzer, L.; Reitenbach, V. Mathematical modeling of unstable transport in underground hydrogen storage. *Environ. Earth Sci.* **2015**, *73*, 6891–6898. [CrossRef]
30. Muhammed, N.S.; Haq, B.; Shehri, D.A.; Al-Ahmed, A.; Rahman, M.M.; Zaman, E. A review on underground hydrogen storage: Insight into geological sites, influencing factors and future outlook. *Energy Rep.* **2022**, *8*, 461–499. [CrossRef]
31. Hemme, C.; Van Berk, W. Hydrogeochemical Modeling to Identify Potential Risks of Underground Hydrogen Storage in Depleted Gas Fields. *Appl. Sci.* **2018**, *8*, 2282. [CrossRef]
32. Kanaani, M.; Sedaee, B.; Asadian-Pakfar, M. Role of Cushion Gas on Underground Hydrogen Storage in Depleted Oil Reservoirs. *J. Energy Storage* **2022**, *45*, 103783. [CrossRef]
33. Aluah, R.; Fadairo, A.; Opeyemi, O.; Ni, R.; Foerster, I. An Experimental Study on the Caprock Integrity of Reservoirs to Assess the Repurposing Depleted Bakken Formation Oil and Gas Fields for Underground Hydrogen Storage. In Proceedings of the SPE Energy Transition Symposium, Houston, TX, USA, 5 August 2024. [CrossRef]
34. Amid, A.; Mignard, D.; Wilkinson, M. Seasonal storage of hydrogen in a depleted natural gas reservoir. *Int. J. Hydrogen Energy* **2016**, *41*, 5549–5558. [CrossRef]
35. Song, H.; Guo, H.; Wang, Y.; Lao, J.; Zhu, H.; Tang, L.; Liu, X. A novel hybrid energy system for hydrogen production and storage in a depleted oil reservoir. *Int. J. Hydrogen Energy* **2021**, *46*, 18020–18031. [CrossRef]
36. Heinemann, N.; Alcalde, J.; Miocic, J.M.; Hangx, S.J.; Kallmeyer, J.; Ostertag-Henning, C.; Hassanpouryouzband, A.; Thaysen, E.M.; Strobel, G.J.; Schmidt-Hattenberger, C.; et al. Enabling large-scale hydrogen storage in porous media–the scientific challenges. *Energy Environ. Sci.* **2021**, *14*, 853–864. [CrossRef]
37. Scafidi, J.; Wilkinson, M.; Gilfillan, S.M.; Heinemann, N.; Haszeldine, R.S. A quantitative assessment of the hydrogen storage capacity of the UK continental shelf. *Int. J. Hydrogen Energy* **2021**, *46*, 8629–8639. [CrossRef]
38. Okoroafor Okoroafor, E.R.; Kim, T.W.; Nazari, N.; Watkins, H.Y.; Saltzer, S.D.; Kovscek, A.R. Assessing the Underground Hydrogen Storage Potential of Depleted Gas Fields in Northern California. In Proceedings of the SPE Annual Technical Conference and Exhibition, Houston, TX, USA, 5 October 2022. [CrossRef]
39. Chen, F.; Ma, Z.; Nasrabadi, H.; Chen, B.; Mehana, M.; Wieke, V.W.J. Technical and Economic Feasibility Analysis of Underground Hydrogen Storage: A Case Study in Intermountain-West Region USA. *arXiv* **2022**, arXiv:2209.03239. [CrossRef]
40. Barison, E.; Donda, F.; Merson, B.; Le Gallo, Y.; Réveillère, A. An insight into underground hydrogen storage in Italy. *Sustainability* **2023**, *15*, 6886. [CrossRef]
41. Yousefi, S.H.; Groenenberg, R.; Koornneef, J.; Juez-Larré, J.; Shahi, M. Techno-economic analysis of developing an underground hydrogen storage facility in depleted gas field: A Dutch case study. *Int. J. Hydrogen Energy* **2023**, *48*, 28824–28842. [CrossRef]
42. Saeed, M.; Jadhawar, P.; Bagala, S. Geochemical effects on storage gases and reservoir rock during underground hydrogen storage: A depleted North Sea oil reservoir case study. *Hydrogen* **2023**, *4*, 323–337. [CrossRef]
43. Okoroafor, E.; Nazari, N.; Kim, T.; Watkins, H.; Saltzer, S.; Kovscek, A. Assessment of hydrogen storage potential in depleted gas fields and power-to-hydrogen conversion efficiency: A northern California case study. *Int. J. Hydrogen Energy* **2024**, *71*, 982–998. [CrossRef]
44. Uliasz-Misiak, B.; Lewandowska-Śmierzchalska, J.; Matuła, R. Hydrogen Storage Potential in Natural Gas Deposits in the Polish Lowlands. *Energies* **2024**, *17*, 374. [CrossRef]
45. Saadat, Z.; Farazmand, M.; Sameti, M. Integration of underground green hydrogen storage in hybrid energy generation. *Fuel* **2024**, *371*, 131899. [CrossRef]
46. Simenson, A.L.; Sonnenberg, S.A.; Cluff, R.M. Depositional facies and petrophysical analysis of the Bakken Formation, Parshall Field and surrounding area, Mountrail County, North Dakota. 2011. Available online: https://repository.mines.edu/handle/11124/16188 (accessed on 20 April 2024).
47. Johanson, K. States with Most Wind Energy. 2021. Available online: https://stacker.com/environment/states-most-untapped-wind-energy-potential (accessed on 20 April 2024).
48. National Energy Technology Laboratory. Underground Hydrogen Storage Remains a Key Research Topic for NETL. Available online: https://netl.doe.gov/node/11982 (accessed on 29 June 2024).
49. Eminoglu, U.; Turksoy, O. Power curve modeling for wind turbine systems: A comparison study. *Int. J. Ambient Energy* **2021**, *42*, 1912–1921. [CrossRef]
50. Dinh, V.D.; Leahy, P.; McKeogh, E.; Murphy, J.; Cummins, V. Development of a viability assessment model for hydrogen production from dedicated offshore wind farms. *Int. J. Hydrogen Energy* **2021**, *46*, 24620–24631. [CrossRef]
51. North Dakota Agricultural Weather Network. Available online: https://ndawn.ndsu.nodak.edu/weather-data-hourly.html (accessed on 19 May 2024).
52. General Electric. 1.5-77 Wind Turbine Brochure. Available online: https://www.energy-xprt.com/downloads/15-77-wind-turbine-brochure-402601 (accessed on 6 October 2024).

53. International Renewable Energy Agency. Hydrogen from Renewable Power Technology Outlook for the Energy Transition. Abu Dhabi. Available online: https://www.irena.org/publications/2018/Sep/Hydrogen-from-renewable-power (accessed on 7 October 2024).
54. North Dakota Department of Mineral Resources. Available online: https://www.ndic.nd.gov/agencies/department-mineral-resources (accessed on 15 June 2024).
55. Pfeiffer, W.T.; Beyer, C.; Bauer, S. Hydrogen storage in a heterogeneous sandstone formation: Dimensioning and induced hydraulic effects. *Pet. Geosci.* **2017**, *23*, 315–326. [CrossRef]
56. Flesch, S.; Pudlo, D.; Albrecht, D.; Jacob, A.; Enzmann, F. Hydrogen underground storage—Petrographic and petrophysical variations in reservoirs and stones from laboratory experiments under simulated reservoir conditions. *Int. J. Hydrogen Energy* **2018**, *43*, 20822–20835. [CrossRef]